Surface & Coatings Technology 203 (2009) 3701–3707

Contents lists available at ScienceDirect

Surface & Coatings Technology

journal homepage: www.elsevier.com/locate/surfcoat

A comparative study of titanium nitrides, TiN, TiNbN and TiCN, as coatings for biomedical applications

A.P. Serro [a,b], C. Completo [a], R. Colaço [c], F. dos Santos [d], C. Lobato da Silva [d], J.M.S. Cabral [d], H. Araújo [e], E. Pires [e], B. Saramago [a,*]

[a] Centro de Química Estrutural, Instituto Superior Técnico, TU Lisbon, Av. Rovisco Pais, 1049-001 Lisboa, Portugal
[b] Instituto Superior de Ciências da Saúde Egas Moniz, Quinta da Granja, Monte da Caparica, 2829-511 Caparica, Portugal
[c] Departamento de Engenharia de Materiais, Instituto Superior Técnico, TU Lisbon, Av. Rovisco Pais 1049-001 Lisboa, Portugal
[d] Institute for Biotechnology and Bioengineering, Centro de Engenharia Biológica e Química, Instituto Superior Técnico, Av. Rovisco Pais 1049-001 Lisboa, Portugal
[e] Ceramed, Azinhaga dos Lameiros (à Estrada do Paço do Lumiar) 1600 Lisboa, Portugal

ARTICLE INFO

Article history:
Received 16 March 2009
Accepted in revised form 3 June 2009
Available online 12 June 2009

Keywords:
Titanium nitride coatings
Friction
Wear
Wettability
Albumin adsorption
Cytotoxicity

ABSTRACT

A strategy used to reduce wear of the ultra high molecular weight polyethylene (UHMWPE) component of orthopedic joint implants has been to coat the metallic part with a hard ceramic layer. The advantage of this procedure is to reduce both wear and ion release of the metal while keeping a high mechanical resistance. In the present study, the performance of three titanium nitride coatings: TiN, TiNbN, and TiCN for biomedical applications was assessed in terms of their surface properties and cytotoxicity. The morphology, chemical composition, and wettability were determined through atomic force microscopy (AFM) imaging, X-ray photoelectron spectroscopy (XPS) and contact angle measurement, respectively. The tribological behaviour of the coatings rubbing against UHMWPE in lubricated conditions was investigated using a pin-on-disk apparatus. Albumin adsorption on the three coatings was studied with a quartz crystal microbalance with dissipation (QCM-D) and AFM scratching. Cytotoxicity was determined both in direct or indirect contact of the cells with the coating materials. The results demonstrate that the three coatings have similar surface properties and are not cytotoxic. TiNbN seems to have the best tribological performance in the presence of albumin, although albumin adsorption is slightly higher on TiN.

1. Introduction

In the last decades, the most widely used prosthesis for total hip and knee replacement involve a metallic part articulating against ultra high molecular weight polyethylene (UHMWPE). However, wear of the polymeric component constitutes a major obstacle limiting the longevity of the implants. Substitution of metal by ceramic has been attempted in order to minimize the wear problem but ceramics have the disadvantage of being brittle with the possibility of suffering catastrophic fracture. Coating of metallic bearing surfaces with ceramics appeared to be a good solution because both wear and ion release are reduced while a high mechanical resistance and a low cost are kept.

Titanium nitrides have been successfully applied as coating materials due to their tribological properties, biocompatibility and affordable price. TiN is one of the most studied ceramic coatings [1–9], however other nitrides such as TiNbN and TiCN may be interesting alternatives. TiNbN is already used in commercially available hip and knee prosthesis but the number of tribological studies of this type of prosthesis reported in the literature is scarce [10–12]. TiCN is widely applied to coat cutting and medical tools [13,14] but, to our knowledge, it was never used to protect the underlying materials in orthopedic prosthesis.

In the present work we present a comparative study of TiN, TiNbN, and TiCN deposited on stainless steel substrates. The objective of the study was to characterize the properties of these materials as extensively as possible in order to provide the conditions for a founded choice of their applications. The morphology, chemical composition, and wettability were assessed through atomic force microscopy (AFM) imaging, X-ray photoelectron spectroscopy (XPS) and contact angle measurements, respectively. The tribological behaviour of the coatings rubbing against UHMWPE in lubricated conditions was investigated using a pin-on-disk apparatus. The biological model fluid Hanks' balanced salt solution (HBSS) and solutions of albumin, the major protein present in the periprosthetic fluid, in HBSS were used as lubricants. Albumin adsorption on the three coatings was determined with a quartz crystal microbalance with dissipation (QCM-D) using coated crystals. AFM data obtained by scratching the adsorbed protein layer with the AFM tip was used to complement the results of the QCM-D technique. Cytotoxicity assays were performed to assess both the cell viability and metabolic activity in direct or indirect contact with the coating materials.

* Corresponding author.
E-mail address: b.saramago@ist.utl.pt (B. Saramago).

0257-8972/$ – see front matter © 2009 Elsevier B.V. All rights reserved.
doi:10.1016/j.surfcoat.2009.06.010

2. Experimental

2.1. Materials

Disks of UHMWPE (CHIRULEN®, Poly Hi Solidur, Germany) with 7 cm of diameter were cut from sheet with 1 mm of thickness for the tribological experiments. Pins of AISI 316L austenitic, stainless steel with 1 cm of diameter were coated with titanium nitride (TiN), titanium niobium nitride (TiNbN), and titanium carbonitride (TiCN). The coatings were deposited by PVD — arc evaporation physical vapour deposition with a METAPLAS coating machine, at 300 °C. The samples were etched with titanium ions at 900 V bias voltage to remove any possible oxide on the surface. In the deposition process the following parameters were used: 200 A cathode deposition current; 100 V bias voltage and 1.4×10^{-2} mbar for the gas pressure. A Ti cathode was used for TiN and TiCN, and a cathode of TiNb alloy, for TiNbN. TiN and TiNbN were produced under nitrogen atmosphere. For TiCN, besides nitrogen, also acetylene was introduced. The thickness of the coatings, measured with a profilometer, varies between 2 and 5 nm. TiN has the lowest hardness (about 22–26 GPa) while the hardness of TiCN and TiNbN are similar and higher than 30 GPa [15].

All substrates were cleaned in an ultrasonic bath with Extran® diluted solution for 10 min and with distilled and deionised water from Milli-Q for 2×10 min and dried overnight at room temperature in a vacuum oven. To test the possibility of water absorption by polymeric substrates, a few were immersed in water for 2 h, but no increase in weight was detected.

The QCM-D studies were done using AT-cut 5 MHz piezoelectric quartz crystals (14 mm in diameter) coated with gold and supplied by KSV Instruments Ltd, Finland. These crystals were coated with TiN, TiNbN and TiCN using the procedure described above for the stainless steel pins. The cleaning procedure used for the crystals was sonication in sodium dodecyl sulfate (3%, from Sigma–Aldrich) followed by double sonication in Milli-Q water for 10 min, and finally blowing dry with nitrogen.

Hank's balanced salt solution — HBSS (Sigma, ref. H8264) and bovine serum albumin — BSA (Serva ref.11930) were used to prepare protein solutions.

Distilled and deionised water was used for measuring static contact angles and in the AFM liquid cell determinations.

3. Methods

3.1. XPS

X-ray photoelectron spectroscopy (XPS) was performed using a VG Scanning Auger Microprobe (Microlab 310F). The spectra were obtained at a pressure of $\approx5\times10^{-9}$ mbar using X-ray from a Mg Kα source (15 kV/20 mA). Chemical identification and determination of relative atomic concentrations were based on the main ionization of the elements obtained with a pass energy of 30 eV. The photoelectrons were analysed at the takeoff angle of 30°. The elemental sensitivity factors were obtained from the VG databank. All the peaks positions were referenced to C 1s at 285.0 ± 0.2 eV. Numerical fitting of the spectra was made using a Gaussian–Lorentzian algorithm. The deconvolution of the peaks was based on reported binding energies [16–20].

3.2. Wettability measurements

The static contact angles were measured through the sessile drop method using a micrometric syringe to generate the drops inside a thermostatized chamber (25 °C) saturated with the corresponding vapour. The images were recorded during 1800 s using an optical equipment described elsewhere [21], and analysed using the Axisymmetric Drop Shape Analysis – Profile (ADSA-P) program [22,23]. The values of the contact angles correspond to the average of at least 10 experiments.

3.3. Afm

A Veeco™ DI CP-II atomic force microscope was used for the topographic characterization. Silicon etched probes, with a nominal radius of 10 nm and a nominal constant of 40 N/m, were used. The imaging was performed in non-contact dynamic mode (NC-mode), at room humidity and temperature conditions. The average roughness, R_a, of the disks was measured over 30×30 μm^2 areas.

To estimate the protein film thickness, the samples were tested under water to avoid protein denaturation using a liquid MicroCell. First, the protein film was removed by performing two scans in contact mode (C-AFM) on areas of 2×2 μm^2. These scans were made with a scan rate of 1 Hz, a 512 lines resolution and a load of 9 μN. This load was found to be sufficient to remove most of the protein film on the stainless steel without any damage of the underlying substrate. Immediately after, 4×4 μm^2 scans were performed with the same probe over the cleaned area, in NC mode, in order to visualize the surface.

The thickness of the films was measured on mean profiles for each scar, considering an average flat reference surface. The position of this reference surface was assumed to be the middle value of the surface asperities height distribution function, retrieved from the surface topographical profile in the region outside the scar. The reported average values of R_a and of film thickness were taken from five different regions in, at least, two different samples.

The preparation of the adsorbed albumin films was carried out by immersion of the samples in the HBSS + BSA solution (10 mg/mL) during 1 h, at room temperature, using a ratio of 4 mL of solution per square centimeter of sample area. After immersion, the samples were rinsed with HBSS to remove unbound protein and dried with nitrogen blowing. For the thickness measurements under water, the samples were transferred to the liquid cell without drying.

3.4. Tribological tests

The tribological experiments were carried out at room temperature on a rotating pin-on-disk tribometer Wazau TRM1000 using HBSS and HBSS + BSA (4 mg/mL) as lubricants. A normal load of 67.5 N was applied which corresponds to a pressure in the contact zone of 0.88 MPa. The tangential sliding velocity was 46 mm/s and the sliding distances were 1000 m. The wear rate of UHMWPE, whose density is 935 kg/m^3, was calculated following a weight loss measurement technique. The results are the average of, at least, three experiments for each system.

3.5. QCM-D measurements

The quartz crystal microbalance with dissipation (KSV Instruments Ltd, Finland, model QCM-Z500) was used to determine BSA adsorption on the surface of the quartz crystals coated with TiN, TiCN and TiNbN.

In order to avoid possible surface contaminations, all the QCM-D balance parts of the measuring cell were sonicated in a 10% alkaline cleaner solution (Extran MA 01), then rinsed in Milli-Q water, and blown dry with nitrogen.

The fundamental frequency along with the third, fifth, seventh, ninth and eleventh harmonics were monitored as a function of time to determine the changes in frequency upon the sequential addition of HBSS, BSA solution and HBSS, to the quartz crystal. The dissipation change was also recorded along the process. The experiments were performed at room temperature. At least three independent measurements were done for each concentration.

Considering the baseline for the first addition of HBSS, the subsequent changes correspond to the formation of a protein layer on the

Table 1
Shear elastic modulus (G), shear viscosity (η) and thickness (t_{QCM-D}) for the BSA film (from [BSA] = 10 mg/mL) obtained by QCM-D.

	G (MPa)	η (mPa s)	t_{QCM-D} (nm)
TiN	0.3 ± 0.1	2.4 ± 0.4	6.6 ± 0.8
TiNbN	0.4 ± 0.2	1.5 ± 0.2	7 ± 2
TiCN	0.4 ± 0.2	1 ± 1	5 ± 3

surface of the crystal followed by a weak removal of adsorbed BSA during rinsing with the solvent. When the viscoelastic properties of the adsorbed film can not be neglected, there are four unknown parameters when modeling the properties of the adsorbed layer, namely thickness, density, elasticity and viscosity. The QCM-D software (QCM-Z500 Data analyser, version 1.62) based on the surface mechanical impedance model allows to model thickness, viscosity and elasticity for a viscoelastic layer whose density is known. Assuming the value of 1.15 g/cm^3 for the density of the adsorbed BSA film [24], the remaining parameters were calculated. As an example, the values of these parameters obtained for [BSA] = 10 mg/mL solutions are given in Table 1.

The BSA adsorption, Γ, was determined using the modified Sauerbrey equation which includes the viscoelastic properties of the adsorbed material [25]:

$$\Gamma = -\frac{\Delta f . C}{n\left(1 - \omega\rho_l\eta_l\frac{J_f''}{\rho_f}\right)} \quad (1)$$

where C has the value of 17.7 ng cm^{-2} Hz^{-1} for the 5 MHz crystals used in this work, n is the number of the harmonic of the fundamental resonance frequency, ω is the angular frequency, ρ_l and η_l are the density and the viscosity of the liquid, respectively, ρ_f is the density of the film and $J_f'' = \frac{\omega\eta_f}{\mu_f^2 + \omega^2\eta_f^2}$, being μ_f, the film elasticity and η_f, the film viscosity.

3.6. Cytotoxicity assays

The coated disks were tested for cytotoxicity following the ISO 10993-5 guidelines. All tested disks were previously sterilised by γ-radiation from a ^{60}Co source, with a dose rate of 30 kGy, using the UTR GAMA-Pi facility. Briefly, each disk type was placed in polystyrene tubes containing 1 mL of RPMI-1640 (a Roswell Park Memorial Institute medium, Gibco B) and kept in an incubator (37 °C, 5% CO_2, fully humidified) for 2 days. The liquid extracts were used to culture L929 mouse fibroblasts (DSMZ, Germany — initial density 80 × 10^3 cells/cm^2) in 24-well plates for 2 days. The cell metabolic activity was determined by analysing the conversion of WST-1 (light red) to its formazan derivative (dark red — absorbance at 450 nm after a 2.5 h incubation at 37 °C) using a WST-1 Cell proliferation kit (Roche). The results were normalized to the negative control for cytotoxicity (fresh RPMI medium) and compared to the positive control (0.01 M Phenol, Sigma). This assay was performed in triplicate.

In order to evaluate the effect of the direct interaction between disks and L929 cells, these were placed on top of a confluent cell layer. At day 3 of culture, cell morphology and death were analysed. Polyethylene (PE) disks were used as a negative control.

Table 2
Surface elemental composition (%) of the TiN, TiNbN and TiCN coatings according to the XPS determinations.

	TiN	TiNbN	TiCN
Ti	30.7	22.8	27.1
N	20.8	20.6	10.3
O	34.1	38.0	41.0
C	14.4	11.5	21.6
Nb	–	7.2	–

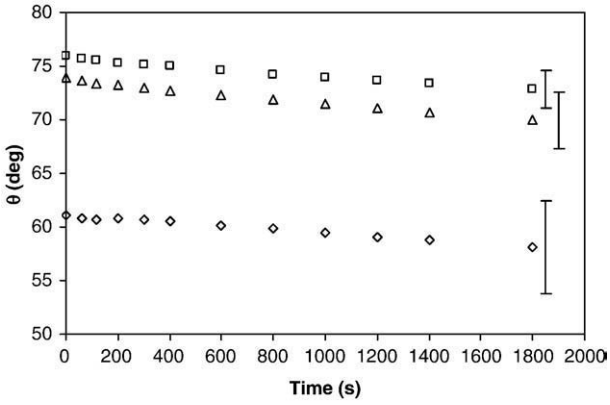

Fig. 1. Static contact angles of water on TiN (◇), TiNbN (□) and TiCN (Δ) as a function of the time.

4. Results and discussion

The surface elemental composition of the three coatings according to the XPS determinations is given in Table 2. The presence of C in samples without carbon in their intrinsic composition is usually associated with organic contaminants while O results from the spontaneous oxidation process of Ti. Fitting of O1s peaks (not shown) showed that, besides the titanium oxide, organic and hydroxyl groups also existed. Comparison of the ratios $O_{(TiO2)}$/Ti indicates that TiNbN is the most oxidized sample which is consistent with the reported decrease of the thermal stability of TiN caused by addition of Nb [26].

The time dependence of the contact angle of water on TiN, TiNbN, and TiCN coatings is shown in Fig. 1. TiNbN and TiCN have similar wettability, while TiN is more hydrophilic.

The dynamical friction coefficients measured in the tests carried out using HBSS and HBSS + BSA are presented in Fig. 2. In the absence of protein, the evolution of the friction coefficient exhibits a running-in period where the friction coefficient increased rapidly and then tended asymptotically to a constant value which is similar for TiN and TiNbN and slightly lower than that of TiCN. Addition of BSA to the lubricant lowers significantly the friction coefficients for the three materials, with special relevance for TiNbN.

Fig. 3 shows the wear rate of the UHMWPE substrates after the tribological tests. No wear could be measured in the counterfaces. The

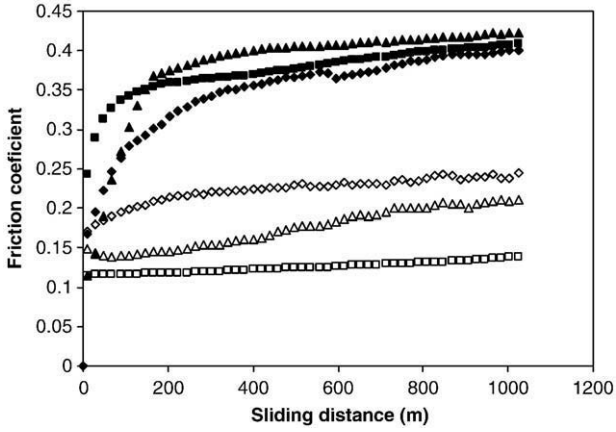

Fig. 2. Friction coefficient versus distance for the tribological pairs TiN/UHMWPE (◆), TiNbN/UHMWPE (■) and TiCN/UHMWPE (▲) in HBSS and TiN/UHMWPE (◇), TiNbN/UHMWPE (□) and TiCN/UHMWPE (Δ) in HBSS + BSA.

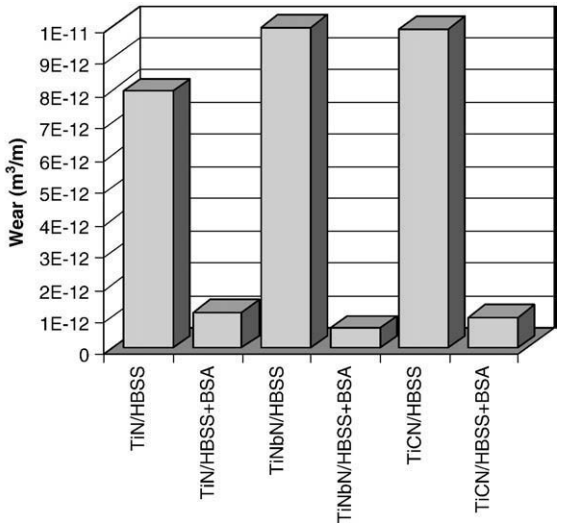

Fig. 3. Wear rate of UHMWPE rubbed against TiN, TiNbN and TiCN in HBSS and HBSS + BSA after 1000 m.

general observation is that polymeric wear against all counterfaces in the presence of protein was much smaller than the corresponding wear in HBSS. Although some dispersion of the results exists, it is fair to conclude that the lowest wear rate was obtained with TiN coating, in pure HBSS, and with TiNbN, in the protein solution.

The main conclusion which can be drawn from the above results is that TiN exhibits the best tribological performance in HBSS, probably due to the lowest value of its hardness. In contrast, when albumin was added to the lubricant, TiNbN seems to be a better choice. The reduction of friction and wear in the presence of protein has been reported by several authors [27,28]. It is attributed to the effect of the adsorbed layer that protects the surface of the tribological pairs leading to the reduction of the interaction between the solid surfaces. This enhances the boundary component of the lubrication and, as a consequence, decreases friction and wear. The change of the wear mechanism from abrasive, when the lubricant is HBSS, to adhesive when BSA is added to HBSS was reported by the authors for the pair TiN/ UHMWPE in a recent work [9].

Adsorption on the coated quartz crystals was investigated in the BSA concentration range 0.05 mg/mL to 15 mg/mL, using the QCM-D technique. The values of Γ on TiN, TiNbN and TiCN-coated quartz crystals obtained from measurements at all harmonics of the fundamental frequency, except $n=1$, are plotted as a function of BSA concentration and compared with two adsorption models in Fig. 4a) and b).

Comparison of our adsorption values with experimental results of other authors is difficult because, to our knowledge, adsorption studies on these materials are practically inexistent. A single value, 1.89 mg/m^2, was reported for TiN which is lower than our lowest value obtained for the most dilute solution ($\Gamma = 2.54$ mg/m^2), however, that measurement was done using radiolabeled albumin added to a plasma solution of unreported protein concentration [1].

The classical models of Langmuir and Freundlich were used to fit the data. Several authors [29–31] found that, although protein adsorption is mostly an irreversible process, their experimental results for BSA adsorption from dilute solutions satisfied the ideal model of Langmuir [32]. According to this theory, Γ, the amount of protein adsorbed per unit surface area of adsorbent, is given by the equation:

$$\Gamma = \frac{a\Gamma_{\max} c}{1 + ac} \tag{2}$$

in which c is the equilibrium concentration of the protein in the bulk solution, $\Gamma_{\max}$ is the maximum value of Γ and a is a constant that compares the rate of adsorption and desorption. Constant a reflects the affinity of the adsorbate molecules toward adsorption sites at a constant temperature. A plot of (c/Γ) versus c should yield a straight line whose slope and intercept lead to the determination of $\Gamma_{\max}$ and a. The parameter a is related to ΔG^{o}_{ads}, the standard Gibbs energy of adsorption, through:

$$a = \frac{1}{c_{solv}} \exp\left(\frac{-\Delta G^{o}_{ads}}{RT}\right) \tag{3}$$

where R is the gas constant, T the temperature, and c_{solv} the molar concentration of the solvent, which was considered for this case as water concentration (55.5 mol/l).

The Freundlich model, though empirical in origin, has been found useful to fit adsorption data onto heterogeneous surfaces [32]. It is given by:

$$\Gamma = kc^{1/n} \tag{4}$$

where k and n are constants that can be obtained from the intercept and the slope of the straight line ln Γ versus ln c. The parameter k is an equilibrium association constant while n indicates the adsorption intensity or surface heterogeneity.

The isotherms calculated with both Langmuir and Freundlich models are compared with the experimental results in Fig. 4a) and b), respectively. The inserts show the fittings to straight lines. Although the correlation coefficients of the linearized Freundlich isotherms are slightly lower than those of the linearized Langmuir isotherms, the former model seems to give a better description of the experimental

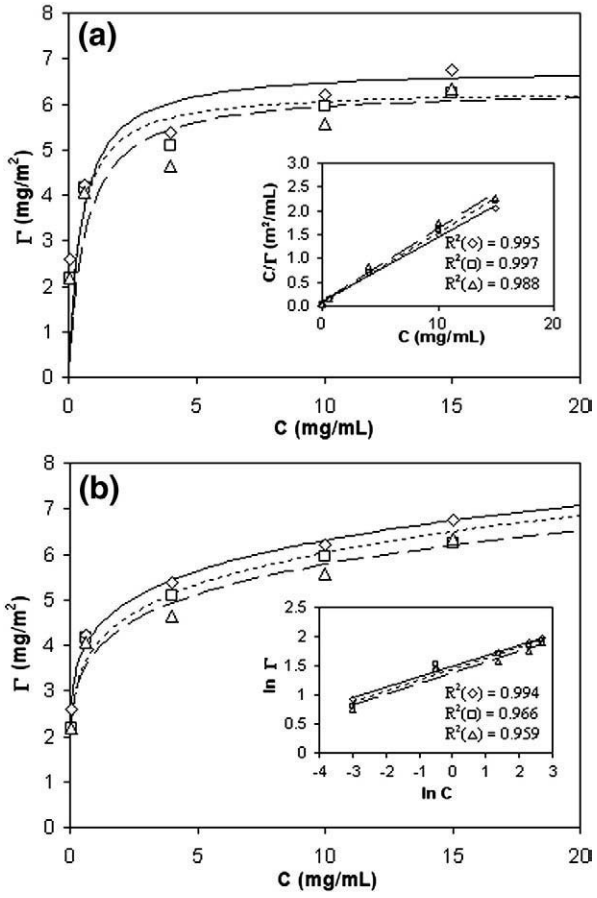

Fig. 4. Adsorption of albumin onto TiN (◇), TiNbN (□) and TiCN (Δ) coatings determined by QCM-D. The lines represent theoretical adsorption isotherms calculated according the Langmuir model (a) and the Freundlich model (b). The inserts represent the linearization data.

Table 3
Fitting parameters to Langmuir (Γ_{max}, a) and Freundlich (k, n) isotherms and ΔG^{o}_{ads} calculated from Eq. (3).

	Γ_{max} (mg/m^2)	a (L/g)	k	n	ΔG^{o}_{ads} (kJ/mol)
TiN	6.78	2.00	4.34	6.16	−39.2
TiNbN	6.32	2.31	3.99	5.56	−39.6
TiCN	6.33	1.56	3.88	5.77	−38.6

values. In fact, the plateau characteristic of the monolayer predicted by the Langmuir model is not attained. Although the Langmuir model has been widely applied to describe protein adsorption, some authors [33] claimed that the empirical Freundlich equation may give a better description of the process. Unlike the ideal Langmuir model which is restricted to the formation of a monolayer, the Freundlich isotherm predicts no limit for adsorption. The steady increase of mass uptake with concentration observed for the three coatings may be attributed to the formation of a multilayer but it can also be due to the increasing amount of water coupled to the protein film.

The parameters obtained from the fittings to the Langmuir and the Freundlich isotherms as well as the standard Gibbs energy of adsorption calculated with Eq. (3) are given in Table 3. The albumin adsorption behaviour on the three coatings is quite similar, although TiN presents slightly higher adsorption. The high negative values of ΔG^{o}_{ads} indicate a strong adsorption onto the surface of the three coatings. The slightly higher value of ΔG^{o}_{ads} for TiN suggests a higher driving force for albumin adsorption on this coating. In general, the driving force for protein adsorption is higher on hydrophobic surfaces than on hydrophilic ones, but, in our case, the difference among the hydrophobicity of the substrates is not relevant and does not allow such a correlation to be established.

Fig. 5 compares the AFM topographic images of the TiN, TiNbN, and TiCN coatings with the images of albumin films adsorbed on these surfaces from [BSA] = 10 mg/mL solutions. The roughness parameters, R_a, of the bare coatings are 8 ± 2 nm. The topography of the protein coated surfaces presents significant changes when compared with the images of the bare coatings, in particular, the surface features of the latter (e.g. polishing scratches) became invisible suggesting that the protein layer covers the whole surface area. Furthermore, the structure of the BSA aggregates can be clearly identified. These aggregates present, in general, a diameter of about 80–150 nm in all the three coatings and tend to exhibit a slightly higher height (about 20 nm) in the TiNbN coating than in the others (<10 nm).

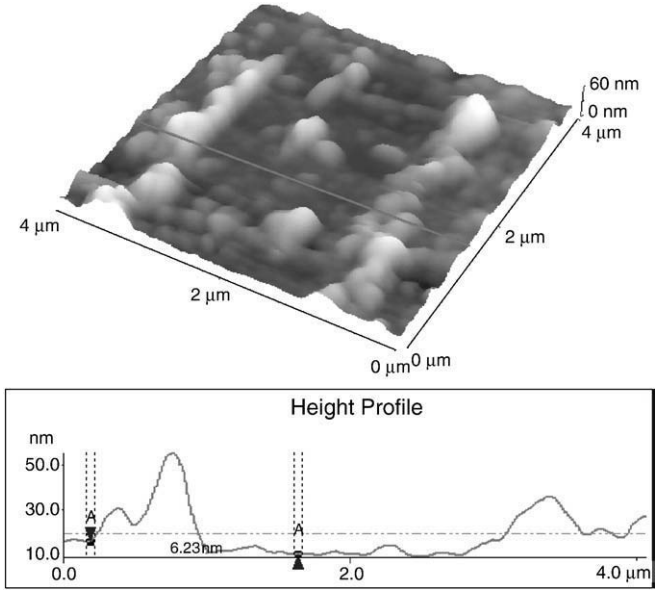

Fig. 6. AFM topographic image, obtained under water, of the scratched area on the protein film adsorbed to the TiNbN coating. A topographic profile is shown beneath the image.

Determination of the thickness of the adsorbed protein layer was made by scratching 2×2 µm^2 squares with the AFM tip. Fig. 6 shows an example of the images under water of the scratched areas on protein films adsorbed on TiNbN and a corresponding topographical line profile from which the thickness of the protein film was estimated. The topographic profiles taken in different regions lead to some natural scatter of the film thickness but, in the three tested coatings, values

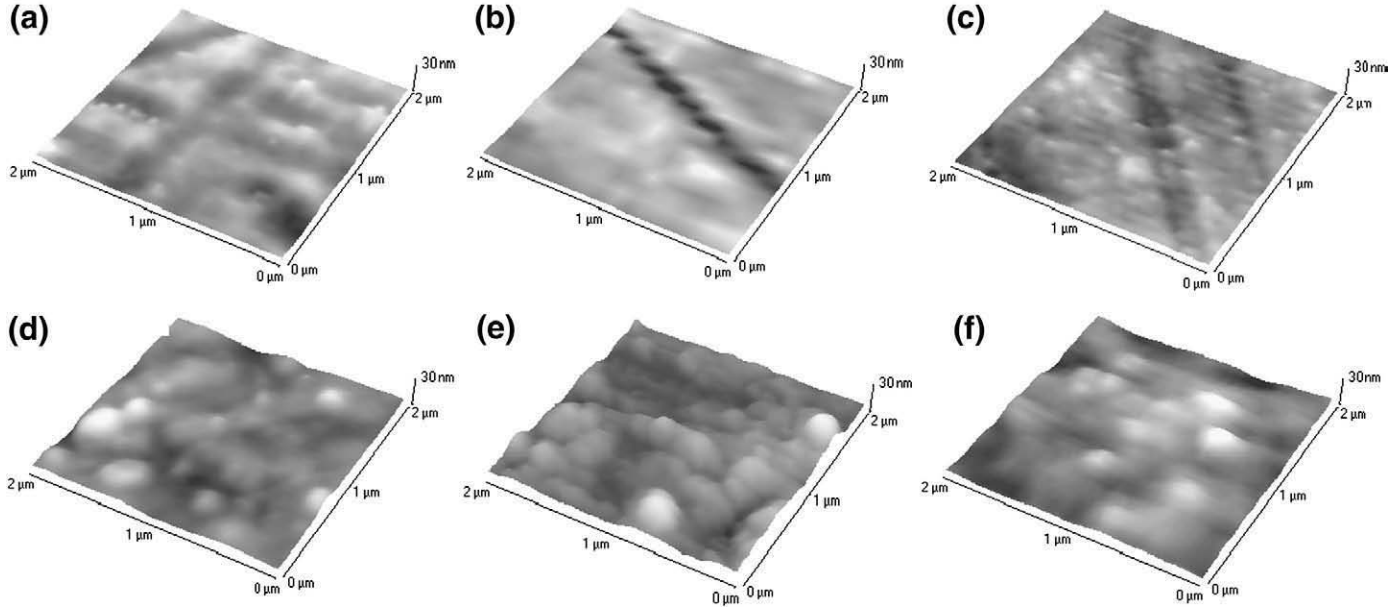

Fig. 5. AFM topographic images (2×2 µm^2) of the (a) TiN, (b) TiNbN and (c) TiCN bare coatings and of albumin films adsorbed on (d) TiN, (e) TiNbN and (f) TiCN coatings. The albumin aggregates are more prominent on the TiNbN coating.

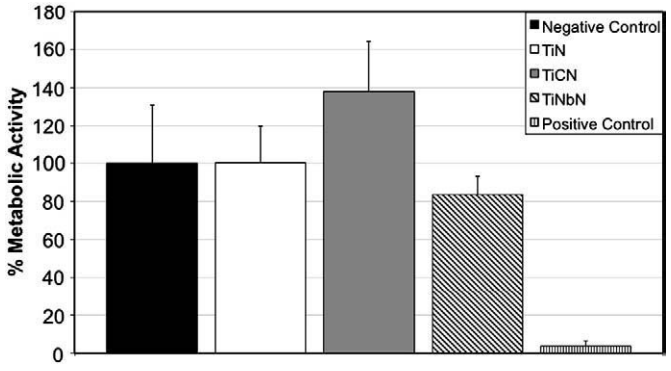

Fig. 7. Indirect contact cytotoxicity assay of stainless coated disks following the ISO standards for biomaterials. Negative control: fresh medium; Positive control: 0.01 M phenol. Results are normalized for the negative control.

between 3 and 8 nm for the thickness of the protein film were obtained from the AFM scratch experiments. These values are in qualitative agreement with those obtained with QCM-D (Table 1) and are compatible with the molecular dimensions of the BSA molecules (heart-shaped configuration, approximated by an equilateral triangle with side ~8 nm and 3 nm of thickness [34]) forming an end-on monolayer or a side-on monolayer.

The adsorption measurements reported above do not allow a direct correlation between the adsorbed amount and/or the affinity of BSA to a particular coating with the improvement of its tribological behaviour when BSA is added to the lubricant. Besides the fact that the observed differences in mass uptake and affinity of albumin to the three coatings are not very significant, other factors such as the viscoelastic properties of the protein layer (see Table 1) may be important. It is interesting to notice that, although TiNbN does not adsorb more albumin than the other coatings, the conformation of the adsorbed protein on its surface seems to be different (see Fig. 5) which may be somehow related with the best tribological performance of the TiNbN coating in the presence of protein.

Finally, cytotoxicity tests were performed with the coating materials for prosthetic implants to test cell responses when interacting with the material. Coated disks were evaluated in terms of cytotoxicity both by indirect and direct contact. Fig. 7 presents the metabolic activity of L929 cells (normalized to negative control) after 48 h of culture with medium extracts of the different coated disks. No cytotoxic effect was observed for any of the materials tested, when compared to fresh culture medium (negative control). In addition, no changes in cell morphology or cell death were visible upon direct interaction with coated disks when compared to polyethylene control disks (as shown in Fig. 8a–d). These results indicate that the coating materials tested are not cytotoxic and may be considered for biomedical applications.

5. Conclusions

In this work the performance of three titanium nitride coatings — TiN, TiNbN and TiCN — for biomedical applications was assessed in terms of their surface properties and cytotoxicity.

The three tested coatings present similar properties. They have similar topography and wettability, although TiN is slightly more hydrophilic.

Friction and wear of polyethylene counterfaces against the three coatings were found to depend on the lubricant: in HBSS, TiN was the best solution while TiNbN seemed to be a better choice when albumin was added to HBSS.

Albumin was found to adsorb strongly on the surface of the three coatings. Adsorption isotherms determined with a quartz crystal microbalance have similar shapes, but the mass uptake is slightly higher for TiN. AFM imaging showed a small difference in the morphology of

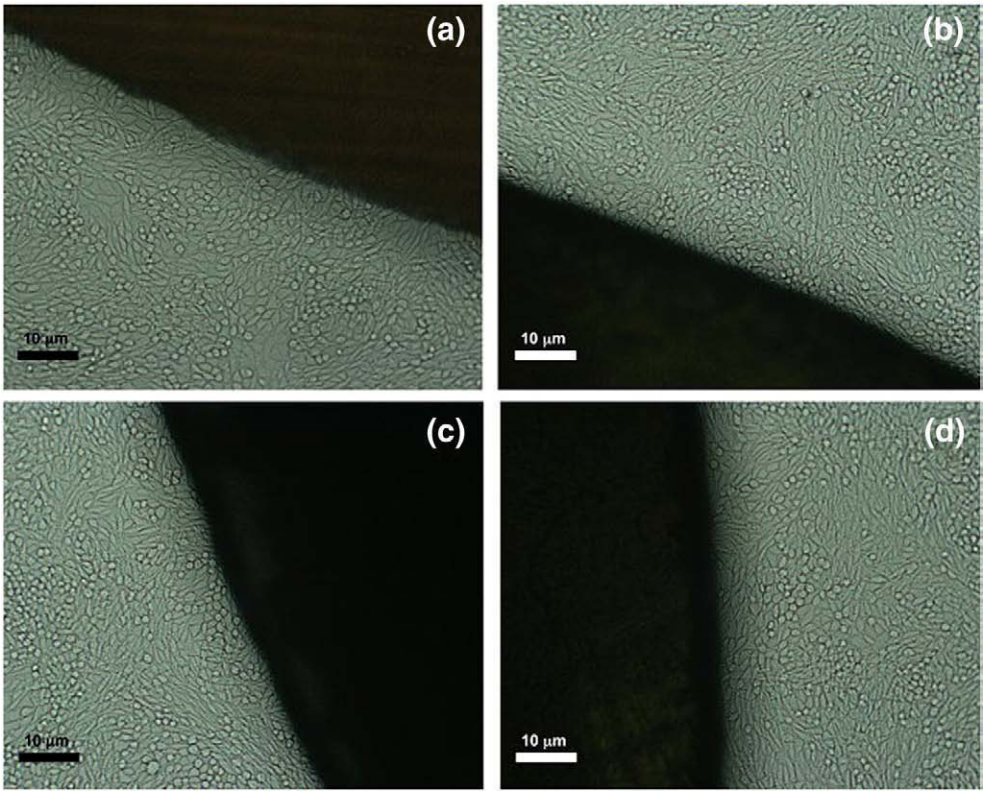

Fig. 8. Direct contact cytotoxicity assay of stainless coated disks following the ISO standards for biomaterials. a) Negative control (PE disks), b) TiN, c) TiCN, d) TiNbN.

the protein layer adsorbed on TiNbN which may be related with its better tribological performance.

All coatings are not cytotoxic and may be used as biomaterials.

Acknowledgments

This study was financially supported by the research project PPCDT /SAU-BMA/55493/2004. The authors are grateful to Luis Ferreira for kindly performing the irradiations in Nuclear Technological Institute of Portugal. A.P. Serro and F. dos Santos acknowledge the Portuguese Foundation for Science for grants SFRH/BPD/5666/2001 and SFRH/BD/38719/2007, respectively.

References

[1] I. Dion, F. Rouais, L. Trut, C. Baquey, J.R. Monties, P. Havlik, Biomaterials 14 (1993) 169.
[2] I. Dion, X. Roques, N. More, L. Labrousse, J. Caix, F. Lefebvre, F. Rouais, J. Gautreau, C. Baquey, Biomaterials 14 (1993) 712.
[3] J. Narayan, W.D. Fan, R.J. Narayan, P. Tiwari, H.H. Stadelmaier, Mat. Sci. Eng. B 25 (1994) 5.
[4] M.T. Raimondi, R. Pietrabissa, Biomaterials 21 (2000) 907.
[5] R. Hubler, A. Cozza, T.L. Marcondes, R.B. Souza, F.F. Fiori, Surf. Coat. Tech. 142 (2001) 1078.
[6] J.I. Oñate, M. Comin, I. Braceras, A. Garcia, J.L. Viviente, M. Brizuela, N. Garagorri, J.L. Peris, J.I. Alava, Surf. Coat. Tech. 142–144 (2001) 1056.
[7] Y. Tamura, A. Yokoyama, F. Watari, T. Kawasaki, Dental. Mat. J. 21 (2002) 355.
[8] E.Y. Gutmanas, I. Gotman, J. Mater. Sci.–Mat. Med. 15 (2004) 327.
[9] M.P. Gispert, A.P. Serro, R. Colaço, A.M. Botelho do Rego, E. Alves, R.C. da Silva, P. Brogueira, E. Pires, B. Saramago, Wear 262 (2007) 1337.
[10] H-G. Neumann, U. Beck, M. Drawe, J. Steinbach, Surf. Coat. Technol. 98 (1998) 1157.
[11] F. Falez, F. La Cava, G. Panegrossi, Int. Orthop. 24 (2000) 126.
[12] M.P. Gispert, A.P. Serro, R. Colaço, E. Pires, B. Saramago, Wear 263 (2007) 1060.
[13] S.J. Bull, D.G. Bhat, M.H. Staia, Surf. Coat. Technol. 163-164 (2003) 507.
[14] J.M. Lackner, W. Waldhauser, R. Ebner, Surf. Coat. Technol. 188–189 (2004) 519.
[15] H. Ljungcrantz, C. Engstrom, L. Hultman, M. Olsson, X. Chu, M.S. Wong, W.D. Sproul, J. Vac. Sci. Tech. A 16 (1998) 3104.
[16] I. Bertóti, M. Mohai, J.L. Sullivan, S.O. Saied, Appl. Surf. Sci. 84 (1995) 357.
[17] C.N. Kirchner, K.H. Hallmeier, R. Szargan, T. Raschke, C. Radehaus, G. Wittstock, Electroanalysis 19 (2007) 1023.
[18] G. Jouve, C. Séverac, S. Cantacuzène, Thin Sol Films 287 (1996) 146.
[19] Y. Dong, Y. Chen, Q. Chen, B. Liu, Z. Song, Surf. Coat. Technol. 201 (2007) 8789.
[20] Y.L. Jeyachandran, S.K. Narayandass, D. Mangalaraj, S. Areva, J.A. Mielczarski, Mat. Sci. Eng. A 445–446 (2007) 223.
[21] W. Ribeiro, J.L. Mata, B. Saramago, Langmuir 23 (2007) 7014.
[22] P. Cheng, D. Li, L. Boruvka, Y. Rotenberg, A.W. Neumann, Colloids Surf. 43 (1990) 151.
[23] P. Cheng, A.W. Neumann, Colloids Surf. 62 (1992) 297.
[24] A.J. Welle, Biomater. Sci. Polymer Edn. 15 (2004) 357.
[25] J. Lukkari, M. Salomäki, T. Ääritalo, K. Loikas, T. Laiho, J. Kankare, Langmuir 18 (2002) 8496.
[26] I.G. Polyakova, T. Hbert, Surf. Coat. Technol. 141 (2001) 55.
[27] M.P. Gispert, A.P. Serro, R. Colaço, B. Saramago, Wear 260 (2006) 149.
[28] M.R. Widmer, M. Heuberger, J. Vörös, N.D. Spencer, Tribol. Lett. 10 (2001) 111.
[29] A. Klinger, D. Steinberg, D. Kohavi, M.N. Sela, J. Biomed. Mater. Res. 36 (1997) 387.
[30] D.R. Jackson, S. Omanovic, S.G. Roscoe, Langmuir 16 (2000) 5449.
[31] M.P. Gispert, A.P. Serro, R. Colaço, B. Saramago, Surf. Interf. Anal. 40 (2008) 1529.
[32] J.D. Andrade, in: J.D. Andrade (Ed.), Surface and Interfacial Aspects of Biomedical Polymers, vol. 2, Plenum Pub., New York, 1985, p. 1.
[33] B. Liu, S. Cao, X. Deng, S. Li, R. Luo, Surf. Sci. 252 (2006) 7830.
[34] W. Norde, C.E. Giacomelli, J. Biotechnol. 79 (2000) 259.